# Impact of Linear-PWM and MPC controllers on the power device losses in a grid-tied two-level inverter

Jose Ortiz Gonzalez[1], Diego Pérez-Estévez[2], Ruizhu Wu[1], Jesús Doval-Gandoy[2] and Olayiwola Alatise[1]

[1]UNIVERSITY OF WARWICK
School of Engineering,
Coventry, United Kingdom
E-Mail:
J.A.Ortiz-Gonzalez@warwick.ac.uk ,
robert.wu.1@warwick.ac.uk ,
o.alatise@warwick.ac.uk

[2]UNIVERSITY OF VIGO
School of Engineering
Vigo, Spain
E-Mail:
dieperez@uvigo.es ,
jdoval@uvigo.es

## Acknowledgements

This work was supported in part by the UK Engineering and Physical Sciences Research Council (EPSRC) through the grant reference EP/R004366/1 and the Spanish State Research Agency under Project PID2019-105612RBQ1I00/AEI/10.13039/501100011033.

## Keywords

«MPC», «PWM», «Grid-connected inverter», «Power semiconductor device», «Power Losses»

## Abstract

This paper presents a comparative analysis of the estimated power losses and device junction temperatures in a two-level grid-tied converter commanded by a linear current controller with a pulse-with-modulator (PWM) or a finite-control-set (FCS) model predictive controller (MPC). This analysis is performed for two points of operation: (a) converter delivering only active power to the grid, (b) exchanging capacitive-reactive power with the grid (STATCOM). Using an electrothermal model based on the firing signals and measured converter currents, the simulation results show the important role of the operating point and control methodology of the converter losses and device junction temperature excursions. The results show that using the MPC controller improves the converter performance when the converter delivers only active power to the grid. In the case of STATCOM operation the total losses are similar, but there is a relative increase of the losses on the diodes. The use of SiC Schottky diodes has been evaluated, with an improvement of the converter performance for both controllers.

## Introduction

The increasing availability and computational power of embedded controllers and an extensive research effort has been fundamental for the emergence and adoption of inverter control methodologies based on optimization techniques, such as model predictive controllers (MPC) [1-4]. Compared with the conventional PWM-based linear current controller [5, 6], MPC controllers offer a fast transient response at a reduced switching frequency, which could be beneficial to grid-tied converters as well as to other applications of power converters.

MPC-based controllers involve the application of optimization techniques. In converter control applications, MPC controllers solve an optimization problem every sampling period for determining the best switching sequence of the converter [4]. Compared to applications with a lower sampling frequency [7, 8], MPC for power converters require a high computational load, which often results in tradeoffs when designing the optimization problem [9]. The controller can be implemented using either a continuous control set (CCS) or a finite control set (FCS). Moreover, novel MPC-based control

methodologies, like [10], are proposed, focusing on achieving a fast time response, low harmonic content with low switching frequencies and a reduced filter size. A constant switching frequency inherent of PWM-controllers may cause high-amplitude harmonics at determined frequencies, which can excite unmodeled resonances in the utility grid [11]. Moreover, when this type of controllers is used, it is possible to obtain low Total Harmonic Distortion (THD) at switching frequencies lower than the typical PWM-based controllers [11]. Traditionally, the low average switching frequency of FCS-MPCs is directly associated with lower losses in the power converter. However, FCS-MPCs present a variable switching frequency, i.e., the number of commutations is not evenly distributed throughout a fundamental cycle of the output voltage. Moreover, the switching frequency also depends on the operating point of the power converter.

From the grid point of view, the main objective is meeting the stringent grid code standards while delivering a reference value of active and reactive power to the grid. In this sense, the impact of the control methodology on the power semiconductor devices of the inverter can be underestimated if only the dynamic response of the current controller is considered, including reference-tracking, disturbance rejection responses and the steady-state harmonic distortion. Studies considering 3-level converters are presented in [12, 13], where the optimization of the control strategy is evaluated for minimizing the thermal stresses on the power devices.

The stresses on the power inverter can be particularly relevant considering the emergence of SiC power semiconductors, with different properties than the conventional silicon power devices. For example, SiC Schottky diodes have negligible switching losses but the conduction losses are higher than for their Si PiN diode counterparts [14]. Simulation studies [15-17] can be very important for understanding the impact of the converter operation on the losses and the resulting junction temperatures of the power semiconductor chips comprising the inverter. These studies can be paramount for device selection during the design phase, hence highly relevant when considering the adoption of SiC power semiconductor devices.

This paper will study the impact of different modulation strategies using two different controllers, namely, a classical PWM-based controller and an MPC controller, on the stresses of the inverter devices at different grid connection power factors. A fast and simple model based on the converter firing signals and the output currents of a 3-phase 2-level inverter is presented as a tool for assisting converter designers in the task of understanding the stresses on the converter and selecting the power semiconductors.

## Control of 2-level grid connected converters

Grid connected converters have to provide the grid with the required active and reactive power while keeping the current harmonic content within the limits defined by the grid code standard. A simplified representation of a grid-connected converter is shown in Fig. 1. For converter designers it is paramount to select the most suitable device and understand the stresses that the different control methodologies will cause on the devices. Fig. 1 shows the block diagram of the controller, the electrical diagram of the 2-level converter and a photograph of the experimental setup used during the experiments.

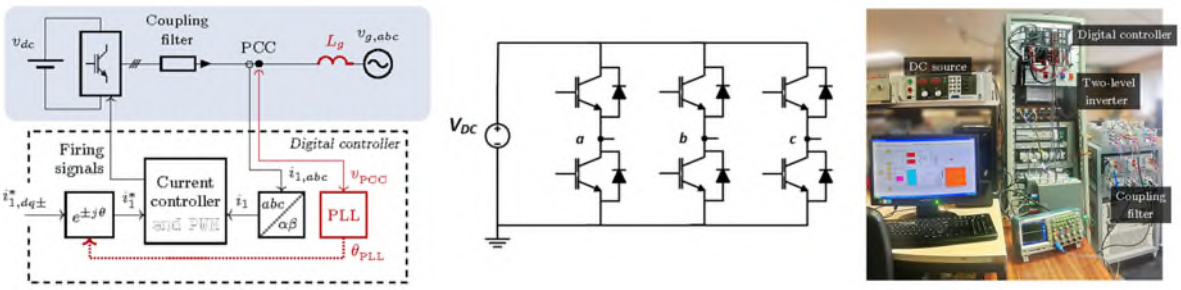


(a) (b) (c)

Fig. 1: (a) Schematic of grid connected converter and controller (b) Two-level inverter (c) Experimental setup

The control of the converter has been implemented using both linear-PWM and MPC current controllers for obtaining the required $i_d$ and $i_q$ currents. On the one hand, the linear-PWM controller selected for the comparison uses a state-space structure with a disturbance observer to achieve zero steady-state error at the fundamental frequency. On the other hand, the MPC current controller selected is a one step-ahead FCS-MPC with delay compensation included in the model. This is a popular choice among researchers and practitioner engineers due to its simple design process and low computational load, compared to more complex MPC designs.

The experimental results are carried out in a 5-kW VSC working as an inverter and connected to a 400 V line-to-line 50-Hz three-phase grid using an L filter (L = 0.3 p.u.). The controller is executed in real-time in an embedded hardware control platform from the German manufacturer dSPACE. The linear-PWM controller [18] is executed at a sampling frequency of 3.6 kHz with a double update sampling strategy that yields a switching frequency of 1800 Hz. The FCS-MPC controller [18] is executed at a sampling frequency of 16 kHz, which results in an average switching frequency of approximately 1800 Hz. The hardware control platform is programmed using Simulink programming language, MATLAB scripts, and C code and it provides a large number of analogue input channels, compared to a traditional oscilloscope. By adding the required external voltage and current sensors, this platform is able to record in the same time base, i.e. simultaneously, the three-phase grid voltages, the three-phase grid currents, and signals internal to the controller such as the VSC firing signals.

The results for the PWM controller are shown in Fig. 2(a) for a purely active power operating point ($i_d$ = 10 A and $i_q$=0 A) and Fig. 3(a) for operation as STATCOM ($i_d$=0 A and $i_q$ = -10 A). Fig. 2(b) and Fig. 3(b) show the gate firing signals for one fundamental cycle. The results clearly show that the grid current and voltages are in phase for the purely active operating point, whereas there is a 90° phase shift between voltage and current in the STATCOM operation. In Fig. 3, the current lags 90° as the current out of the converter has been defined as positive.

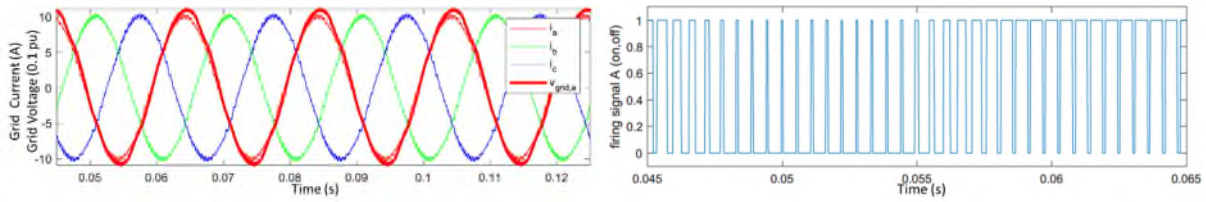


(a) (b)

Fig. 2 PWM controller, Purely Active Power operation(a) Grid currents and phase A voltage (b) Firing Signal phase A

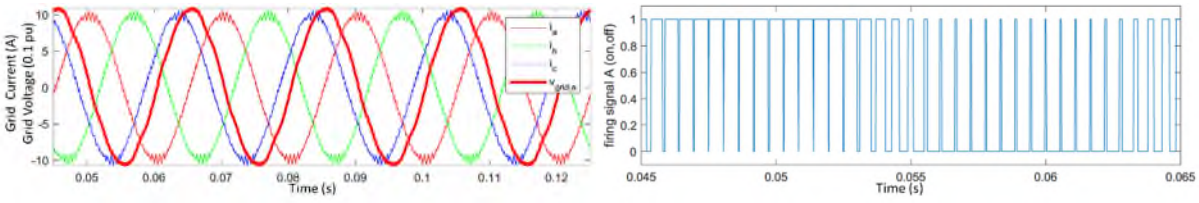


(a) (b)

Fig. 3 PWM controller, STATCOM operation (a) Grid currents and phase A voltage (b) Firing Signal phase A

The control of the converter can also be implemented using MPC techniques. The change of the state of the firing signal is determined by an optimization function [4], which decides the optimal converter output state for achieving the required grid currents and voltages.

It is important to mention that MPC and MPC-FCS controllers that do not use a PWM vary their average switching frequency depending on the modulation index. The modulation index of a converter depends on the relation between DC bus voltage and the amplitude of the three-phase voltage generated at the inverter output. For the comparative analysis presented in this paper, these values are adjusted to obtain

the same average switching frequency for both controllers. The results are shown in Figs. 4 and 5, for the same operating points.

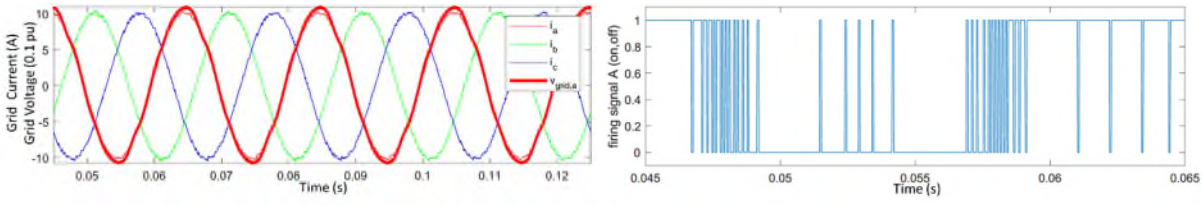


(a) (b)

Fig 4 MPC controller, Purely Active Power operation (a) Grid currents and grid phase A voltage (b) Firing Signal phase A

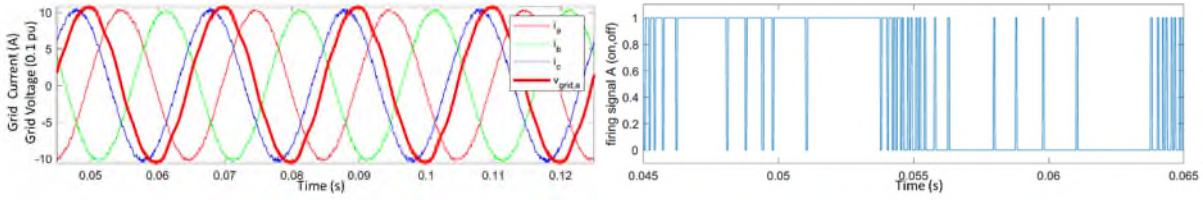


(a) (b)

Fig 5 MPC controller, STATCOM operation (a) Grid currents and grid phase A voltage (b) Firing Signal phase A

Compared with the conventional PWM current controller in Fig. 2 and Fig. 3, the firing signals include longer periods where the device is ON. In this situation the conduction losses of the power device will dominate, and the thermal performance will be affected. The next sections will evaluate how this affects the converter loss distribution.

## Converter model and device loss implementation

The evaluation of the power device losses within a converter is an area of increasing interest, as it can help converter designers to evaluate the impact of different mission profiles on the converter performance [16, 20]. A simulation model for its evaluation is used in this paper for evaluating the impact of the operating point of the converter on the conduction and switching losses.

There are different methods for obtaining the conduction and switching losses, including analytical methods, simulation models and look-up tables (LUTs) based on datasheet parameters or experimental measurements [15, 16, 21, 22]. The device selected for evaluation is a 1.2 kV Si IGBT with datasheet number IKW25T120 and a current rating of 25 A at 100 °C. The switching performance of the device has been evaluated using the co-packaged Si PiN diode and a 1200 V SiC Schottky diode with datasheet number C4D10120A and a current rating of 23 A at 100 °C.

For this investigation, the ON-state losses have been extracted from the device datasheets whereas the switching losses have been experimentally characterized using a double pulse test set-up [23], for a set of temperatures and load currents, using both the Si PiN diode and the SiC Schottky diode. The experimental converter waveforms were obtained using a converter that uses power devices different from the previously mentioned devices. Nevertheless, the analysis method presented in this paper is suitable for a quick converter evaluation that can assist converter designers to understand the loss distribution within the converter for optimizing the device selection.

Using the experimentally measured currents and firing gate signals (conceptual plots shown in Fig. 6), it is possible to calculate the resulting conduction and switching losses [22], as shown in Fig. 7. It is important to highlight that the sampling rate of the gate firing signals has to be high enough to be able to capture the short duration ON and OFF pulses. The sampling time used in this paper is 2 µs. which is

short enough to accurately simulate the junction temperature though the actual switching time is even shorter.

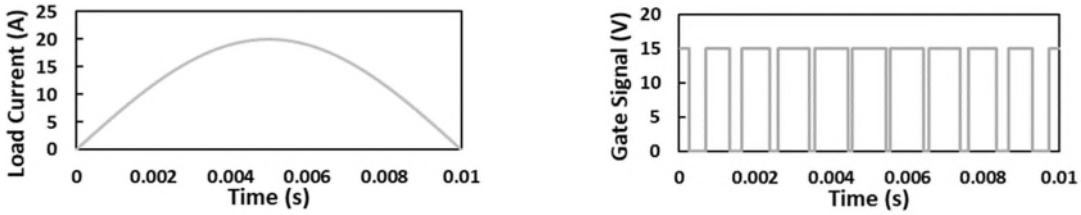


(a) (b)

Fig. 6 PWM Modulation – Conceptual plots. (a) Load current and (b) gate firing signal

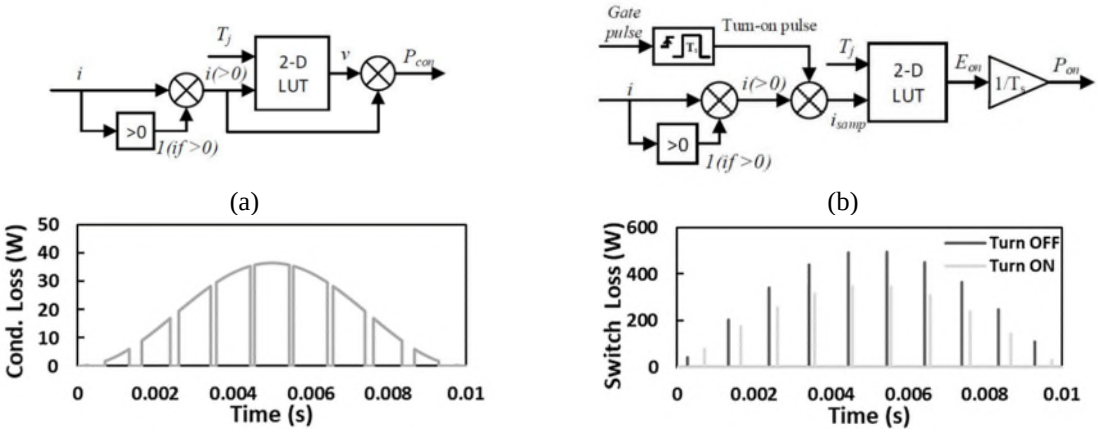


(a) (b)

(c) (d)

Fig. 7: (a) Transistor conduction and (b) Turn-ON switching loss calculation. Conceptual diagrams for (c) Conduction losses and (d) Switching losses

When the phase current is negative, the current flows through the antiparallel Si PiN diode or SiC Schottky diode, hence the losses of the diodes are easy to calculate using loss calculator for the diode, shown in Fig. 8 (a). The turn-OFF of the diode occurs when the complementary transistor in the leg switches ON. SiC Schottky diodes do not have reverse recovery losses and the switching losses can be neglected. However, that is not the case of Si PiN diodes, where the reverse recovery energy has to be considered. The reverse recovery was determined experimentally using a double pulse test circuit [23], for a range of currents and temperatures, populating the look-up table in Fig. 8(b).

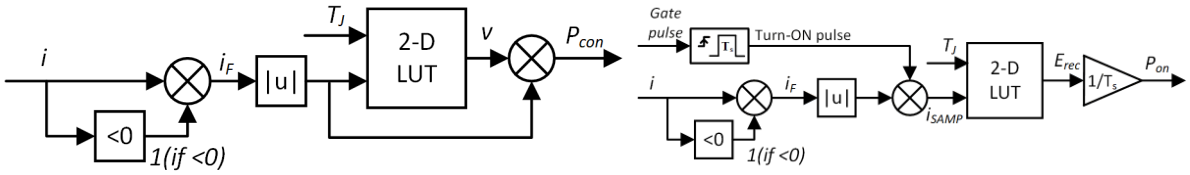


(a) (b)

Fig. 8: Conduction and switching loss calculation of the diode – (a) Conduction and (b) Switching loss calculation

This methodology is fast to implement and could enable the rapid evaluation of the operating point on the converter loss distribution, as it will be demonstrated in the next section

## Impact of the operating point on the loss distribution in grid tied converters

The point of operation (power factor) will play a key role on the loss distribution of the power devices in the inverter and it can be fundamental for the selection of the most suitable power device. This has been evaluated using the model proposed in the previous section. The firing signals were obtained using a DC link voltage of 600 V and the switching frequency was fixed at 1800 Hz for the PWM controlled

converter. In the case of the MPC controller, the frequency is dependent of the DC link voltage and for this study, the DC link was adjusted to obtain an average switching frequency equal to the PWM controller.
A case temperature of 100 °C was considered for the simulation analysis and the junction temperatures are calculated using the thermal network provided by the manufacturer, as described in [22]. The results of the loss and junction temperature calculations for the PWM- and MPC-controlled Si IGBT/Si PiN inverters are presented in the next sections.

## Impact of the operating point in a PWM-controlled Si IGBT/Si PiN inverter

The total loss per phase, device loss distribution and resulting junction temperature excursions of the Si IGBT and Si PiN diode are shown in Fig. 9 for the operating point in Fig. 2 ($i_d$ = 10 A and $i_q$ = 0 A) and Fig. 10 for the operating point in Fig. 3 ($i_d$=0 A and $i_q$ = -10 A).

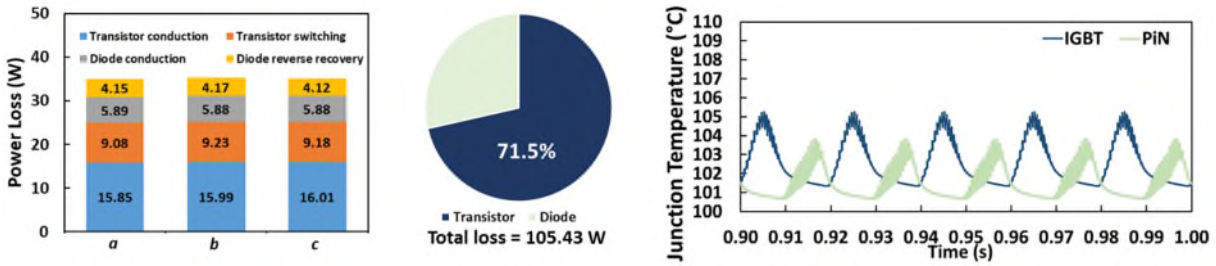


Fig. 9: Si IGBT/Si PiN inverter, PWM controller. Purely Active Power operation. Losses and junction temperature excursion

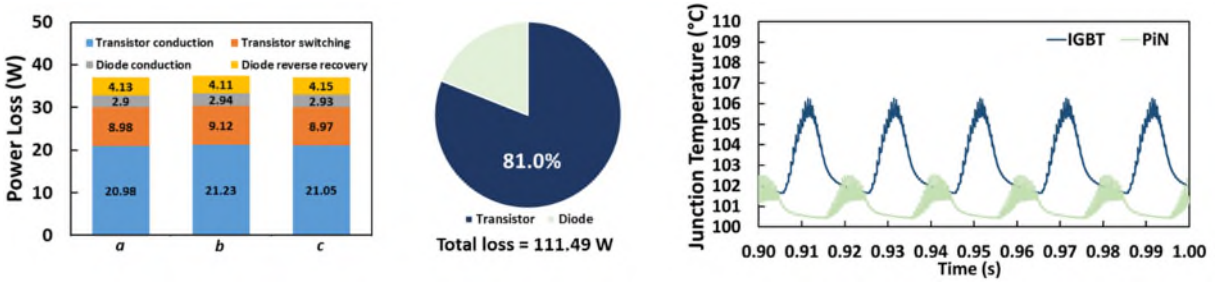


Fig. 10: Si IGBT/Si PiN inverter, PWM controller. STATCOM operation. Losses and junction temperature excursion,

The results in Figs. 9 and 10 clearly demonstrate the impact of the point of operation on the converter losses. In the case of the purely reactive case, as a result of the higher conduction losses in the IGBT, the total losses increase 5.7% and the share of the IGBTs is now 81%. The results also show a reduction of the conduction losses on the silicon PiN diode. This is reflected in the junction temperature excursions of the devices, which will have implications on the lifetime of the power devices [24, 25].

## Impact of the operating point in a MPC controlled Si IGBT/Si PiN inverter

As mentioned previously, the DC link was adjusted to obtain the same average switching frequency the PWM controller; hence, a correction factor was applied to the switching losses, based on the information provided on the datasheet of the device. The calculated losses and junction temperature excursions for the MPC controller in the same operating points than the PWM controller, namely purely active power and STATCOM operation, are shown in Fig. 11 and Fig. 12 respectively.

The results for the MPC show that for the purely resistive load ($i_d$=10 A and $i_q$ = 0 A), the share of the losses of the IGBT is 85.3% with the conduction losses of the IGBT playing a fundamental role. Considering the purely reactive load, the total losses increase 18.5% and, more important, the losses on the Si PiN diode now represent a 39.5% of the total loss because of the increased share of conduction losses. This is clearly reflected on the junction temperature excursions in Fig. 12 (STATCOM operation) which shows the impact of the higher thermal resistance of the PiN diode compared with the IGBT, resulting in higher junction temperature excursions.

Additionally, an interesting observation from the measured waveforms in Fig. 4 and Fig. 5 is that in the case of the Purely Active power the switching commutations happen at low current levels, whereas in the case of the STATCOM operation, the switching events occur at high current levels. This is reflected in the IGBT switching losses in Fig. 11 and Fig. 12.

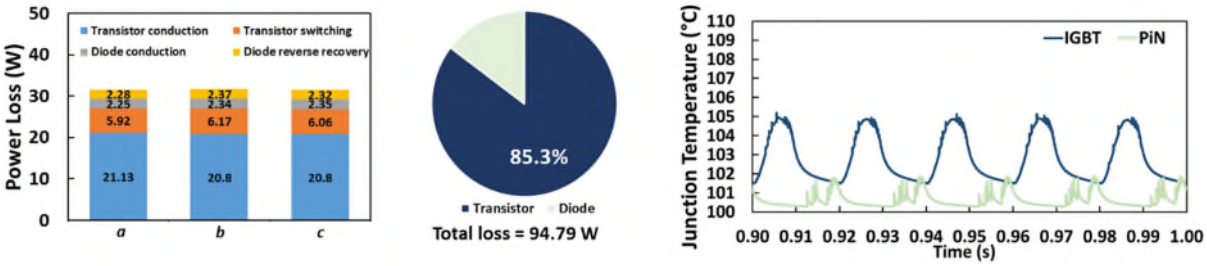


Fig. 11: Si IGBT/Si PiN inverter, MPC controller. Purely Active Power operation. Losses and junction temperature excursion

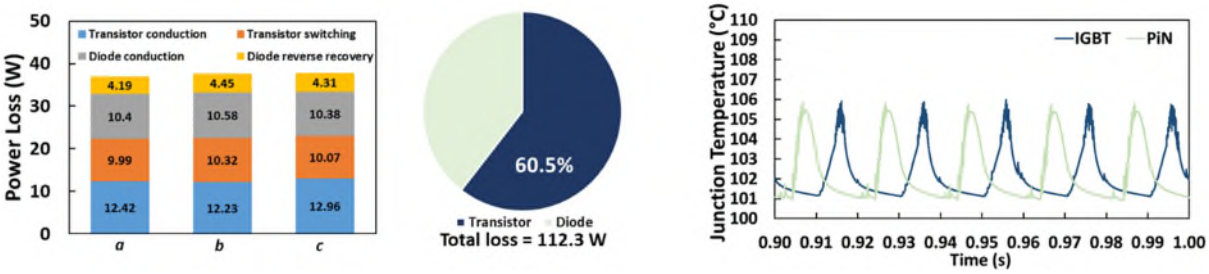


Fig. 12: Si IGBT/Si PiN inverter, MPC controller, STATCOM operation. Losses and junction temperature excursion

## Impact of SiC diodes on PWM and MPC controlled converters

SiC Schottky diodes present negligible switching losses that are not affected by temperature [14, 26], however the conduction losses are higher than in Si PiN diodes. This highlights the importance of the operating point of the converter when selecting a device technology. The impact of replacing the Si PiN diode with a SiC Schottky diode is evaluated for both pure active power generation and STATCOM operation in a Si IGBT/SiC Schottky inverter in this section of the paper.

### Purely Active Power - Si IGBT/SiC Schottky inverter

First, the impact of replacing the Si PiN diode with a SiC Schottky is evaluated in the case of purely active power generation. The results are shown in Fig. 13 and Fig. 14 for the PWM and MPC controller respectively. The results clearly show that the use of SiC Schottky diodes improves the performance of the converter. In the case of the PWM controller, comparing Fig. 9 (Full Si) and Fig. 13, a reduction of 12.7% of the total losses is observed, as well as improvement on the junction temperature excursions. In the case of the MPC controller (Fig. 11 and Fig. 14), there is an improvement of 9.1% on the total losses.

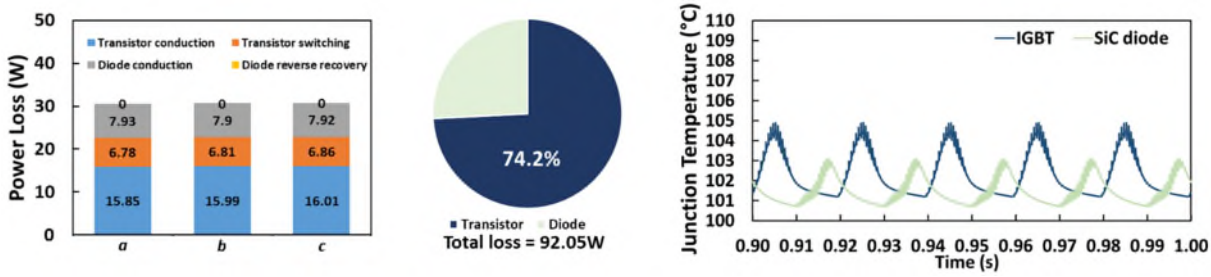

Fig.13 Si IGBT/SiC diode, PWM controller. Purely Active Power operation. Losses and junction temperature excursion

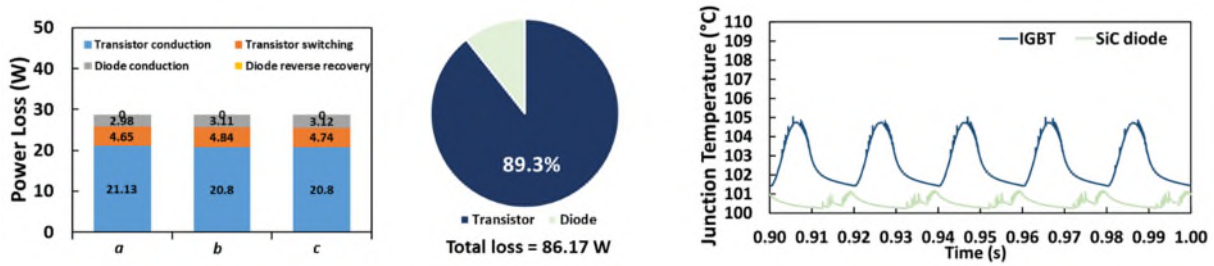


Fig.14 Si IGBT/SiC diode, MPC controller, Purely Active Power operation. Losses and junction temperature excursion

### STATCOM operation - Si IGBT/SiC Schottky inverter

The same comparison has been performed in the case of STATCOM operation and the results for the converters with SiC Schottky diodes are shown in Fig 15 and Fig 16 for the PWM and MPC controller respectively.

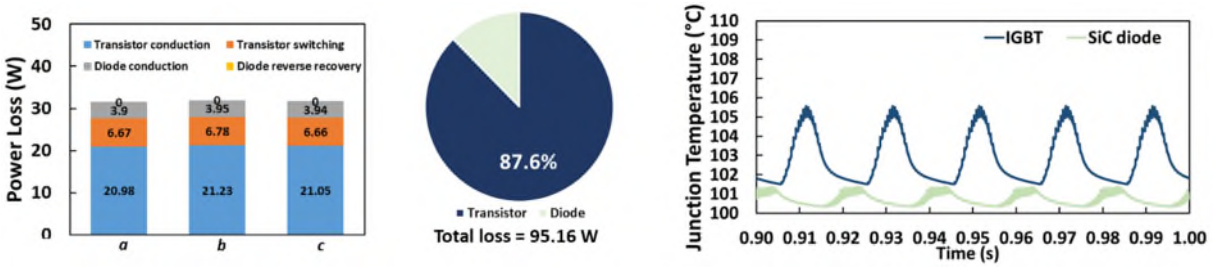


Fig.15 Si IGBT/SiC diode, PWM controller. STATCOM operation. Losses and junction temperature excursion

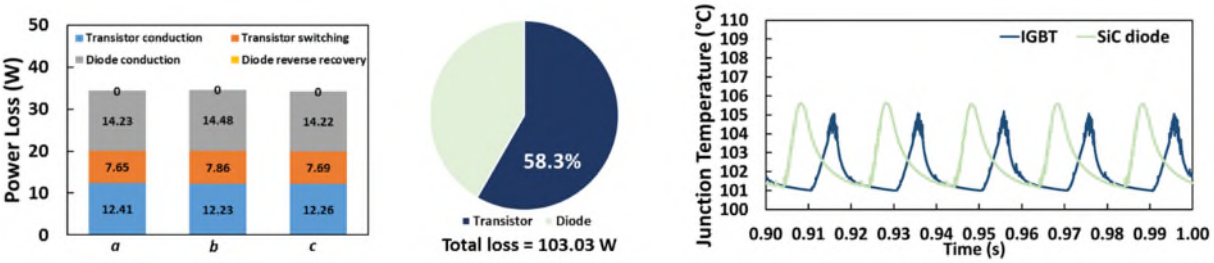


Fig.16 Si IGBT/SiC diode, MPC controller, STATCOM operation. Losses and junction temperature excursion

Comparing the results of the Si IGBT/SiC Schottky inverter with the Si IGBT/Si PiN inverter the use of SiC Schottky diodes shows an improvement of the converter performance. In the case of the PWM controller, comparing Fig. 10 (Full Si) and Fig. 15, a reduction of 14.7% of the total losses is observed, as well as improvement on the junction temperature excursion, more apparent in the case of the diode. In the case of the MPC controller (Fig. 12 and Fig. 16), there is an improvement of 8.2%, as the improved switching loss performance is compensated with the higher conduction losses of the Schottky diode

## Conclusion

This paper has evaluated the impact of PWM and MPC current controllers in the performance of a 2-level grid tied converter using a model with fast simulation times. Using the firing signals and measured converter currents, it is shown that the point of operation plays a key role on the converter losses as a function of the current controller used. The results show improved performance of the MPC

controlled converter when the converter delivers only active power to the grid whereas for operation as STATCOM losses in diodes are higher and lower in transistors, although total losses are similar. The use of SiC Schottky diodes can be fundamental for improving the converter performance of both controllers.

## References


[1] P. Karamanakos, E. Liegmann, T. Geyer, and R. Kennel, "Model Predictive Control of Power Electronic Systems: Methods, Results, and Challenges," *IEEE Open Journal of Industry Applications*, vol. 1,pp. 95-114, 2020.

[2] S. Vazquez, J. Rodriguez, M. Rivera, L. G. Franquelo, and M. Norambuena, "Model Predictive Control for Power Converters and Drives: Advances and Trends," *IEEE Transactions on Industrial Electronics*, vol. 64, no. 2, pp. 935-947, 2017.

[3] Y. Zhang, J. Liu, H. Yang, and S. Fan, "New Insights Into Model Predictive Control for Three-Phase Power Converters," *IEEE Transactions on Industry Applications*, vol. 55, no. 2, pp. 1973-1982, 2019

[4] J. Rodriguez, J. Pontt, C. A. Silva, P. Correa, P. Lezana, P. Cortes, *et al.*, "Predictive Current Control of a Voltage Source Inverter," *IEEE Transactions on Industrial Electronics*, vol. 54, no. 1, pp. 495-503, 2007.

[5] J. Kukkola and M. Hinkkanen, "State Observer for Grid-Voltage Sensorless Control of a Converter Under Unbalanced Conditions," *IEEE Transactions on Industry Applications*, vol. 54, no. 1, pp. 286-297, 2018.

[6] X. Wang, M. G. Taul, H. Wu, Y. Liao, F. Blaabjerg, and L. Harnefors, "Grid-Synchronization Stability of Converter-Based Resources—An Overview," *IEEE Open Journal of Industry Applications*, vol. 1, pp. 115-134, 2020.

[7] S. A. Bonab and A. Emadi, "MPC-Based Energy Management Strategy for an Autonomous Hybrid Electric Vehicle," *IEEE Open Journal of Industry Applications*, vol. 1,pp. 171-180, 2020.

[8] D. Dewar, J. Rohten, A. Formentini, and P. Zanchetta, "Decentralised Optimal Controller Design of Variable Frequency Three-Phase Power Electronic Networks Accounting for Sub-System Interactions," *IEEE Open Journal of Industry Applications*, vol. 1,pp. 270-282, 2020.

[9] P. Karamanakos and T. Geyer, "Guidelines for the Design of Finite Control Set Model Predictive Controllers," *IEEE Transactions on Power Electronics*, vol. 35, no. 7, pp. 7434-7450, 2020.

[10] X. Chen, W. Wu, N. Gao, H. S. H. Chung, M. Liserre, and F. Blaabjerg, "Finite Control Set Model Predictive Control for LCL-Filtered Grid-Tied Inverter With Minimum Sensors," *IEEE Transactions on Industrial Electronics*, vol. 67, no. 12, pp. 9980-9990, 2020.

[11] D. Pérez-Estévez and J. Doval-Gandoy, "A Finite-Control-Set Linear Current Controller With Fast Transient Response and Low Switching Frequency for Grid-Tied Inverters," *IEEE Transactions on Industry Applications*, vol. 56, no. 6, pp. 6546-6564, 2020.

[12] A. A. Rockhill, M. Liserre, R. Teodorescu, and P. Rodriguez, "Grid-Filter Design for a Multimegawatt Medium-Voltage Voltage-Source Inverter," *IEEE Transactions on Industrial Electronics*, vol. 58, no. 4, pp. 1205-1217, 2011.

[13] E. Kantar and A. M. Hava, "Optimal Design of Grid-Connected Voltage-Source Converters Considering Cost and Operating Factors," *IEEE Transactions on Industrial Electronics*, vol. 63, no. 9, pp. 5336-5347, 2016.

[14] ROHM, *SiC Power Devices and Modules Application Note* Rev.003, 2020

[15] A. Bryant, N. Parker-Allotey, D. Hamilton, I. Swan, P. A. Mawby, T. Ueta, *et al.*, "A Fast Loss and Temperature Simulation Method for Power Converters, Part I: Electrothermal Modeling and Validation," *IEEE Transactions on Power Electronics*, vol. 27, no. 1, pp. 248-257, 2012.

[16] L. Ceccarelli, R. M. Kotecha, A. S. Bahman, F. Iannuzzo, and H. A. Mantooth, "Mission-Profile-Based Lifetime Prediction for a SiC MOSFET Power Module Using a Multi-Step Condition-Mapping Simulation Strategy," *IEEE Transactions on Power Electronics*, vol. 34, no. 10, pp. 9698-9708, 2019

[17] Z. Davletzhanova, O. Alatise, J. O. Gonzalez, S. Konaklieva, and R. Bonyadi, "Electrothermal Stresses in SiC MOSFET and Si IGBT 3L-NPC Converters for Motor Drive Applications," in *PCIM Europe 2017;* pp. 1-8.

[18] D. Pérez-Estévez, J. Doval-Gandoy, A. G. Yepes, Ó. López and F. Baneira, "Generalized Multifrequency Current Controller for Grid-Connected Converters With LCL Filter," in *IEEE Transactions on Industry Applications*, vol. 54, no. 5, pp. 4537-4553, Sept.-Oct. 2018

[19] D. Perez-Estevez and J. Doval-Gandoy, "A Model Predictive Current Controller With Improved Robustness Against Measurement Noise and Plant Model Variations," in *IEEE Open Journal of Industry Applications*, doi: 10.1109/OJIA.2021.3074502.

[20] K. Ma, M. Liserre, F. Blaabjerg, and T. Kerekes, "Thermal Loading and Lifetime Estimation for Power Device Considering Mission Profiles in Wind Power Converter," *IEEE Transactions on Power Electronics*, vol. 30, no. 2, pp. 590-602, 2015.

[21] R. Yuancheng, X. Ming, Z. Jinghai, and F. C. Lee, "Analytical loss model of power MOSFET," *IEEE Transactions on Power Electronics*, vol. 21, no. 2, pp. 310-319, 2006.

[22] R. Wu, J. O. Gonzalez, Z. Davletzhanova, P. A. Mawby, and O. Alatise, "The Potential of SiC Cascode JFETs in Electric Vehicle Traction Inverters," *IEEE Transactions on Transportation Electrification*, vol. 5, no. 4, pp. 1349-1359, 2019.

[23] J. O. Gonzalez, R. Wu, S. Jahdi, and O. Alatise, "Performance and Reliability Review of 650 V and 900 V Silicon and SiC Devices: MOSFETs, Cascode JFETs and IGBTs," *IEEE Transactions on Industrial Electronics*, vol. 67, no. 9, pp. 7375-7385, 2020.

[24] U. Choi, F. Blaabjerg, and S. Jørgensen, "Study on Effect of Junction Temperature Swing Duration on Lifetime of Transfer Molded Power IGBT Modules," *IEEE Transactions on Power Electronics*, vol. 32, no. 8, pp. 6434-6443, 2017.

[25] B. Hu, J. O. Gonzalez, L. Ran, H. Ren, Z. Zeng, W. Lai, *et al.*, "Failure and Reliability Analysis of a SiC Power Module Based on Stress Comparison to a Si Device," *IEEE Transactions on Device and Materials Reliability*, vol. 17, no. 4, pp. 727-737, 2017.

[26] J. Hu, O. Alatise, J. O. Gonzalez, R. Bonyadi, L. Ran, and P. Mawby, "Comparative electrothermal analysis between SiC Schottky and silicon PiN diodes: Paralleling and thermal considerations," in *2016 18th European Conference on Power Electronics and Applications (EPE'16 ECCE Europe)*, 2016, pp. 1-8